WHITE PAPER

How to Design User Equipment Antenna Systems for 5G Wireless Networks

Next-generation cellular wireless communications will enable numerous innovative, cutting-edge technologies and products. The combination of millimeter-wave (mm-wave) and microwave bands accompanied by advanced spatial multiplexing techniques such as massive multiple-input multiple-output (MIMO) will form the backbone of a new cellular technology called 5G. The evolution to 5G promises low latency, high data rates and increased channel capacity for mobile communication networks. Delivering this promise requires revamping existing networks, building new infrastructure and developing the client devices. These are major changes and implementing them is going to be difficult, costly and time-consuming. To this end, virtual prototyping through simulation can help solve the difficult engineering challenges, realize innovations and reduce costs. Despite the importance of simulation, not much work or literature is available describing comprehensive modeling workflows for creating 5G wireless designs and systems and characterizing end-to-end wireless networks. This paper provides pervasive simulation techniques and workflows for designing 5G antennas, microcell arrays and end-user devices or user equipment (UE) on Ansys tools. The workflows include human-device interaction to analyze the effectiveness of a hand-held UE and to ensure that the UE design does not overstep regulations.

Figure 1. 5G will enable a fast and whole new connected world

/ The Potential and Challenge of 5G

5G will bring revolutionary changes to mobile communications with a 100X increase in channel capacity, 20 Gbps peak data rates and a 10X drop in latency to a few milliseconds. It will drive innovation, enable the creation of exciting products and services with far-reaching impact on many industries. Its low latency and highly reliable networks will be crucial for ensuring safe operation of autonomous vehicles, when they hit the road. In addition to enhanced performance of the vehicle-to-vehicle (V2V) and vehicle-to-infrastructure (V2I) communications, 5G will boost many aspects of the Internet of Things (IoT). Its massive connectivity and high capacity networks can expand the scope of IoT to enable smart cities.

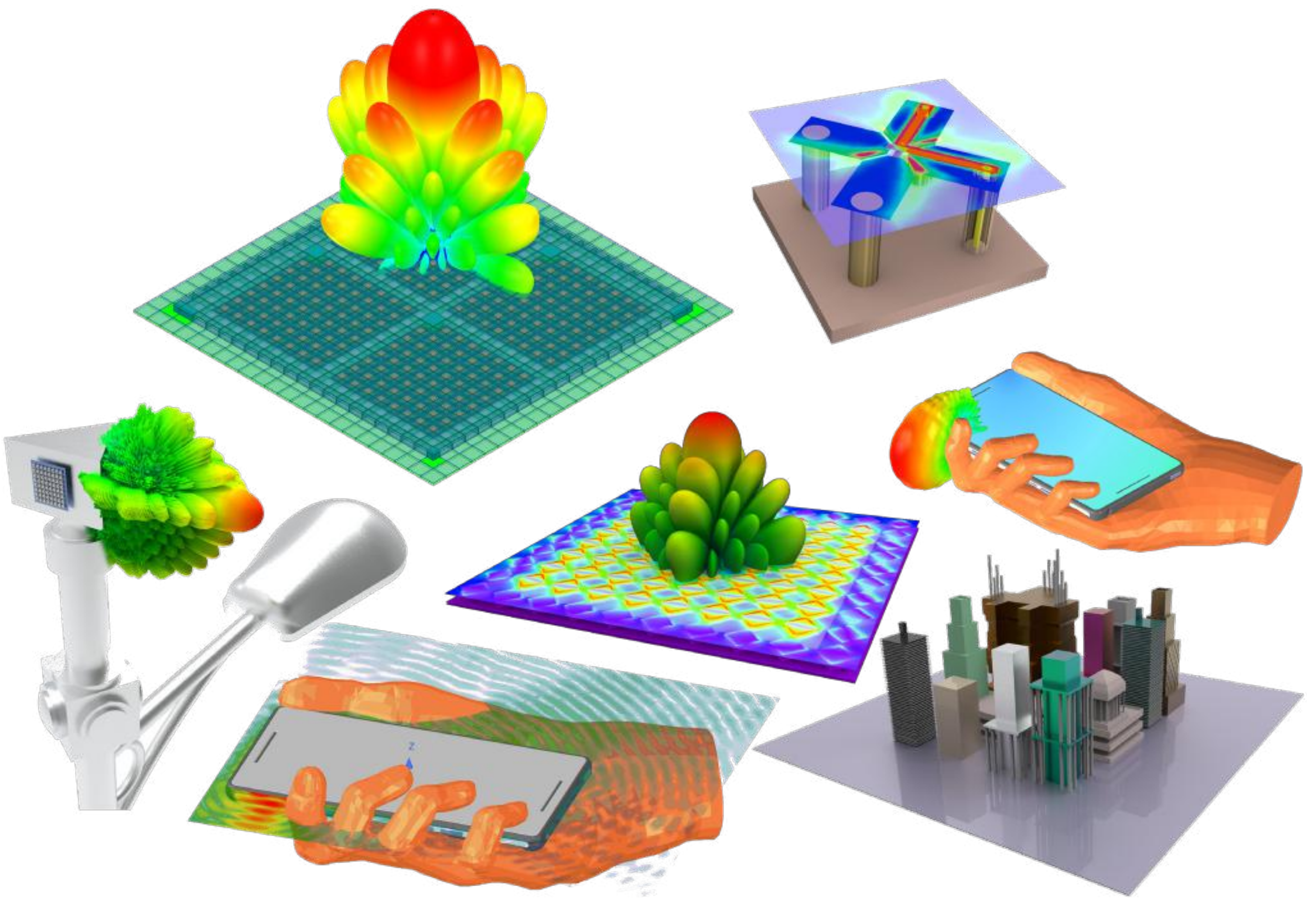

Figure 2. Ansys HFSS: A versatile 3D EM design and simulation tool for wireless and electronic systems

5G will utilize millimeter-wave bands while leveraging sub-6 GHz frequencies through carrier aggregation (CA). The millimeter-wave (mm-wave) band has its merits and demerits. It provides large bandwidth, low latency, high data rate and increased channel capacity. However, simultaneous multi-band RF and digital signals being present within the same wireless device can be problematic leading to RF interference issues. These issues can be due to unwanted out-of-band emissions by the collocated RF systems as well as by broadband noise and harmonics generated by the digital signals that couple into the victim receiver of a wireless system. These problems can become increasingly pronounced as more and more ICs, System-on-Chips (SoCs), packages, and wireless systems are integrated on a single 5G device.

Design considerations of a 5G network utilizing mm waves are not just limited to the performance of the antennas, user equipment, microcell and the propagation channels. They should also consider the interactions of mm-waves with a human body since that could give rise to potential biocompatibility issues of the user equipment.

Since the millimeter-wave frequency has shorter wavelength than current 4G frequency bands, the number of antenna elements in a 5G microcell array can be increased to fit more elements within the same space. An array with more elements allows selective power delivery through spatial beamforming capabilities. It also permits the use of advanced massive multiple input multiple output (MIMO) beamforming techniques. That said, designing a large mm wave array poses stiff challenges starting from the antenna, building the array, modeling its interaction with the radome and weight-matrix computation for beamforming.

The design and optimization of the UE and microcell cannot be optimally achieved in isolation. Both are tied to the communication channel, defined as the propagation medium between the antennas of the UE and microcell. Electromagnetic waves propagate in this channel and carry signals between the UE and microcell. At present, existing channel estimation techniques are utilized to model and extract the channel state information (CSI) between a microcell and UE. These estimation techniques are based upon theoretical work examined and verified using empirical data which are already available for sub-6 GHz wireless communications. For characterizing mm-wave channels, the current estimation techniques cannot be used without modifications. The modifications are necessary to account for the severe path loss that mm waves undergo from absorption, blockage and reflection along the signal propagation channel. Simulation tools employing ray tracing techniques are suitable to account for the multiple reflections, bounces, phase delays and losses experienced by the mm waves in a complex environment. Both ray tracing techniques as well as statistical models and techniques can be used to compute the CSI for mm-waves.

/ End User Device or User Equipment (UE) Design

User equipment covers a wide range of wireless consumer electronics devices. Typical UE examples are smartphones, tablets, medical devices, and smartwatches or for that matter any IoT device. The UE discussed in this paper is a smartphone. 5G mobile phones will be required to operate in the new mm-wave and sub-6 GHz 5G bands in addition to the previous generation of wireless technologies (4G LTE and earlier). Smartphones must accommodate multiple antennas that can provide GPS, GSM and LTE services.

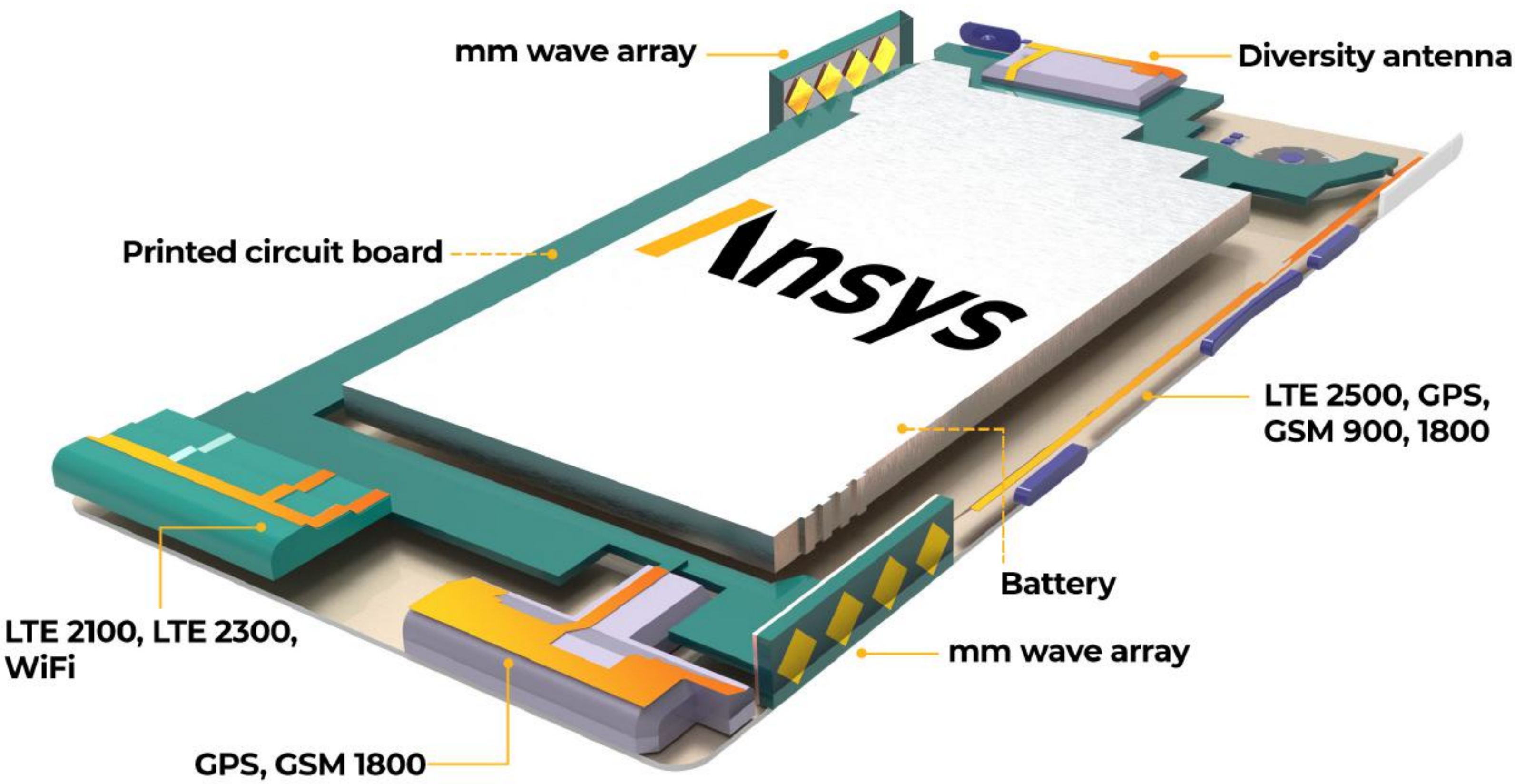

Figure 3. Internal details of a Smartphone in HFSS

To enhance coverage and provide reliable wireless communications, smartphones generally utilize the spatial diversity scheme with multiple antennas placed at different edges/corners of the phone. To exploit the spatial diversity scheme, a 5G smartphone usually has a collection of antennas that are physically separate from one other. **Figure 3** is a virtual prototype of a typical smartphone showing its internal details.

/ Integrated Antenna Design at Sub-6 GHz

Ansys HFSS offers a systematic workflow to design sub-6 GHz integrated antennas intended for LTE, 4G, GSM and GPS services. Three types of antennas are designed to operate at GSM 900, Wi-Fi, LTE 2100, 2300, GPS, GSM 1800 and LTE 2500 bands.

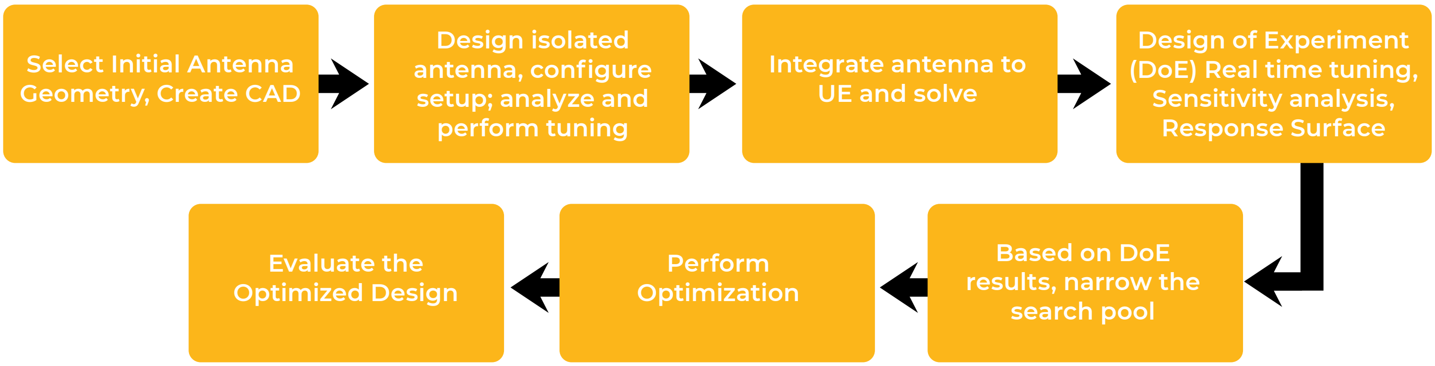

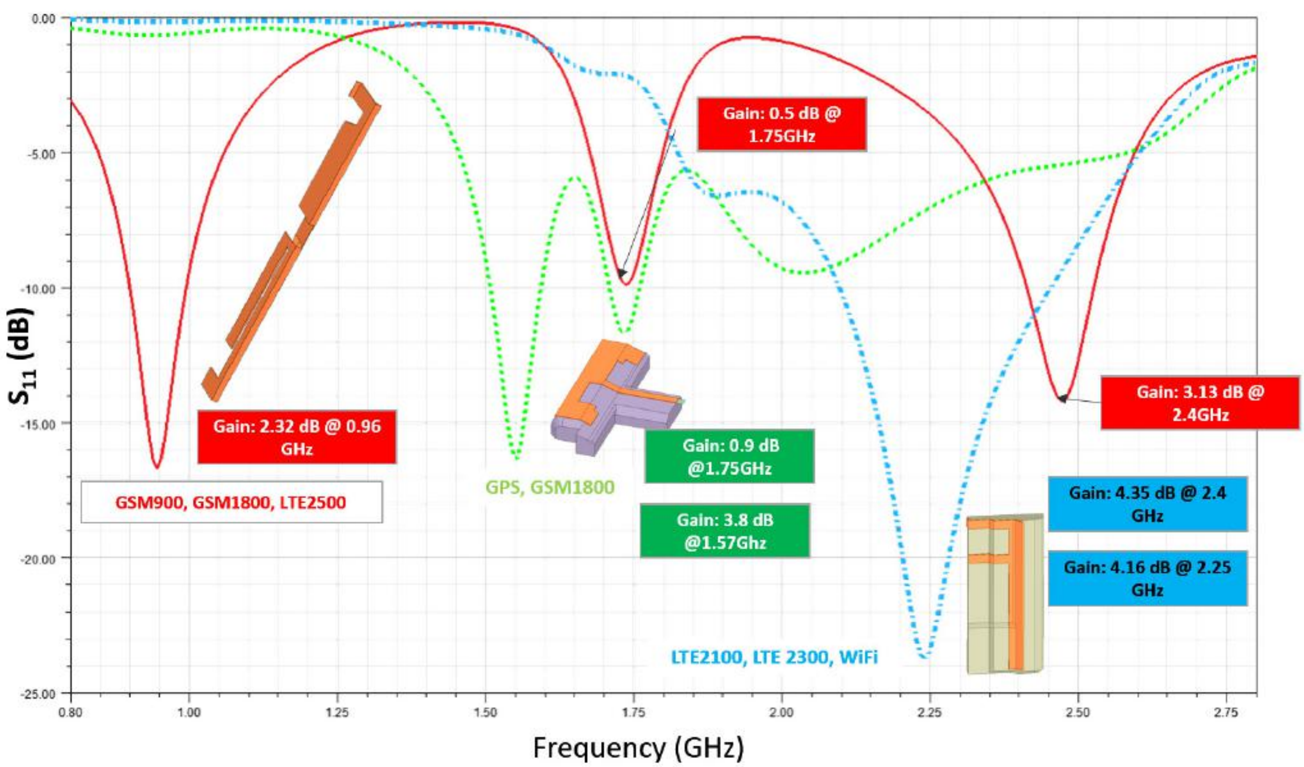

Figure 4. Sub-6 GHz antennas designed in Ansys HFSS

Using a good rule of thumb, an initial 3D model is created for each antenna. Three types of antenna are chosen: a planar inverted F antenna (PIFA), T-shape monopole and 3D blade monopole antenna. Each antenna is independently analyzed in HFSS, tuned and integrated into the phone. The full assembly is then simulated. As expected, the integration of the antennas into the phone model impacts their performance. To achieve the desired antenna gain and input impedance, Design-Of-Experiments (DoE) methods are applied simultaneously for all the three antennas. Based on the results, a narrow search pool is created from the variables having highest impact on the desired outputs. An optimization algorithm is invoked to search through the pool and find the best combination of variables. **Figure 4** shows the return loss plots for the final antenna designs. The evaluated reflection coefficients and realized gain are shown in their appropriate plots. **Figures 4** and **5** show the realized peak gain values and radiation patterns at different frequencies.

/ Integrated Millimeter-Wave Array for UE

A similar workflow (as described for sub 6 GHz antennas) is used to design the integrated mm wave array. The frequency band of interest for the array is 26–28.5 GHz. These frequencies belong to the Ka-band mm-wave sub-bands that are being considered for 5G (bands n257, n258, n260 and n261). Each element of the mm-wave array is a microstrip patch with two probe feeds. The substrate is 1.376 mm thick and assigned the material Roger RT/Duroid 5870 (dielectric constant = 2.33, dielectric loss tangent = 0.0012). A passive parasitic stacking patch is added to improve the operational bandwidth. The model is designed to operate within the frequency band of interest: 26.5 GHz–28.8 GHz.

Each microstrip patch element has two feeds, and supports both vertical (V) as well as horizontal (H) polarizations. Each antenna is optimized to operate at the defined band with a reasonable return loss of less than -10dB (S11<-10 dB). On placing the individual antennas in succession along a straight line, an array is generated. The array is then integrated into the phone. At various stages of the design, from the initial element to the array and its final integration onto the phone, it is important to properly tune the antenna. Tuning the antenna and the array improves their efficiency and ensures that the electronics within the device and its housing do not decrease the array's performance.

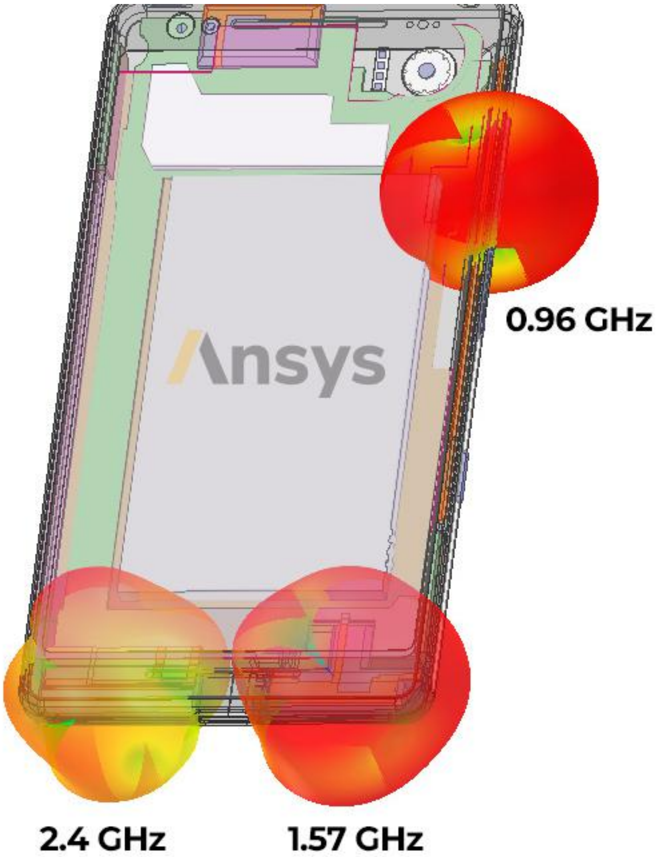

Figure 5. Phone with radiation patterns

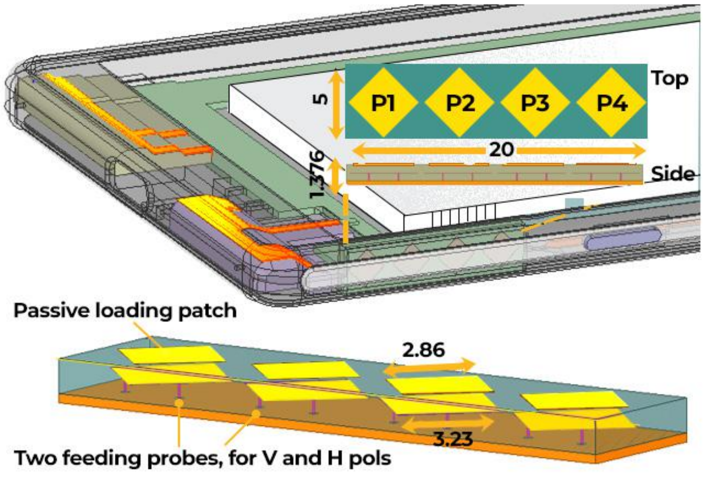

Figure 6. A 4x1 patch array with dual polarization (V,H), sub-strate Roger RT/Duriod 5870 (units: mm): stacked patch for bandwidth

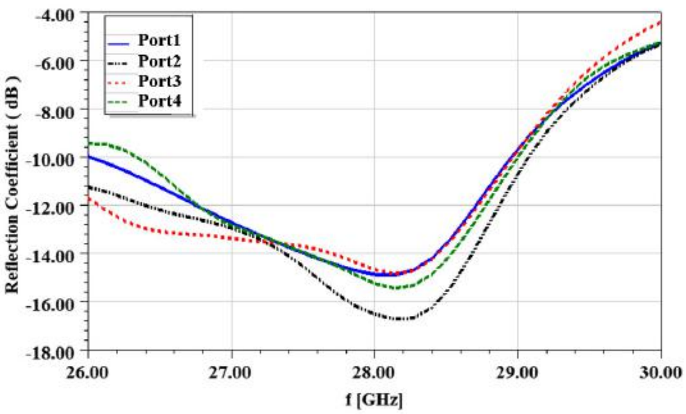

Figure 7. Reflection coefficient of Array1 integrated with the phone. Four V-pol ports are excited (H-pol are terminated).

Figure 6 shows a portion of the final design. **Figure 7** shows the reflection coefficient of the array for V-pol excitation.

To automate the complete simulation, a GUI (or ACT) extension using a Python script is integrated into Ansys Electronics Desktop. The extension adds a 5G Wizard toolkit in Electronics Desktop to load the HFSS design and import all the excitation data through a plain text file (*.CSV). The toolkit is convenient since it allows all excitations to be automatically assigned to the antenna elements. It also makes it easy to calculate the radiation pattern of the array for each beam ID. Additionally, it facilitates calculations of the cumulative distribution function (CDF) and power density values for the design automatically in HFSS.

/ Beam Codebook

To compensate for the severity in path loss of mm-waves, it is important to maximize beamforming in the intended direction so that a stable communication link is established and maintained between a UE and microcell. The smaller wavelength allows mm-wave arrays to be considerably scaled-down to fit inside a UE. The elements of the array are excited with varying magnitudes and phases to produce different beam directions. By creating a linear progressive phase shift between the elements, the main beam scans from the broadside (for zero phase shift between elements) toward the end-fire (with 180 degrees phase shift between elements). This beamforming capability increases the array's gain and allows the beam to be focused in the desired direction to overcome the propagation loss. The array's beamsteering capabilities allow a wider area to be scanned, thus improving the transmission and/or signal reception.

Standard beam codebooks comprising a set of beam IDs or codewords are available for given antenna configurations. A codeword could be a set of complex values of excitations expressed in terms of their magnitudes and phases. A simple example of a codebook is Table 1 for a 4x1 array design. Different formats of the codebook can be imported to HFSS. Based on the Beam ID, the parameters in the Edit Sources dialog in HFSS are updated to reflect the excitations of the array elements. The full-wave radiation pattern for each beam ID is then calculated. In this way, the performance and accuracy of the codebook can be examined and verified, without need to repeat electromagnetic simulation for each beam position.

Beam ID	Port 1	Port 2	Port 3	Port 4
1	1W @ 0°	1W @ -145°	1W @ -290°	1W @ -435°
2	1W @ 0°	1W @ -84°	1W @ -168°	1W @ -252°
3	1W @ 0°	1W @ 0°	1W @ 0°	1W @ 0°
4	1W @ 0°	1W @ 84°	1W @ 168°	1W @ 252°
5	1W @ 0°	1W @ 145°	1W @ 290°	1W @ 435°

Table 1: Beam ID Codebook data is supplied in *.CSV format to the 5G wizard in HFSS

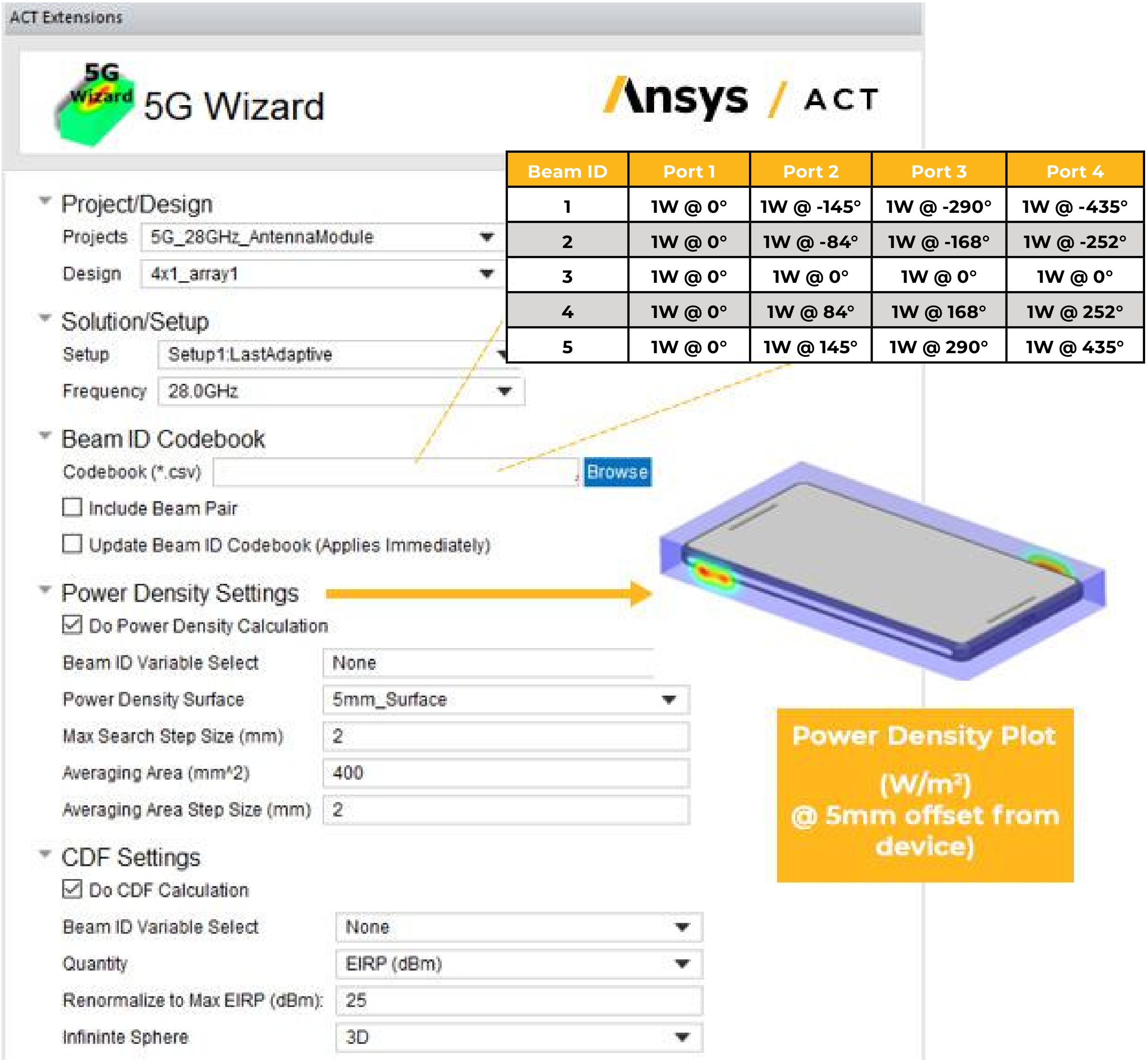

Beam ID	Port 1	Port 2	Port 3	Port 4
1	1W @ 0°	1W @ -145°	1W @ -290°	1W @ -435°
2	1W @ 0°	1W @ -84°	1W @ -168°	1W @ -252°
3	1W @ 0°	1W @ 0°	1W @ 0°	1W @ 0°
4	1W @ 0°	1W @ 84°	1W @ 168°	1W @ 252°
5	1W @ 0°	1W @ 145°	1W @ 290°	1W @ 435°

Figure 8. 5G wizard in HFSS

/ Power Density

Any wireless consumer electronics device must comply with various criteria and meet FCC or EU regulatory standards and rules to ensure user safety. As an example, the FCC mandates the Specific Absorption Rates (SAR) for devices operating in the sub-6 GHz band be below the stipulated values in order to limit the RF exposure to users. In the mm-wave band, where the wave energy is mainly focused at the surface (due to skin effect), power densities of these devices are a more suitable and commonly used metric for complying with FCC regulations. Using the Ansys 5G Wizard in Electronics Desktop, the power density (PD) corresponding to each beam ID for a selected surface is computed based on the following equation:

$$PD = \frac{\iint_A E \times H * ds}{A}$$

/ Cumulative Distribution Function

The 3rd Generation Partnership Project (3GPP), as the 5G standardization body, specifies the minimum peak equivalent isotropic power (EIRP) requirement for handheld UE.

Quantitatively, EIRP is expressed in terms of the realized array gain as follows:

$$EIRP = P^{inc} . G_{realized}(w_c, \theta, \varphi)$$

where P^{inc} is the total incident power supplied to the array elements. As the expression shows, optimizing for the realized gain is the same as optimizing for EIRP. Here, for simplicity, the incident power is normalized.

In a given θ and $\varnothing$ direction, $G_{realized}$ is the maximum value of the array's gain over the set of codewords w_c. In other words, $G_{realized}$ is an aggregate gain pattern representing the peak gain across all beams. This is the maximum gain that the array will deliver in any given direction and corresponds to the codeword that will be selected by the electronics driving the antenna array deployed in the field.

The 3GPP standard specifies the spherical coverage requirements for 5G UE (power class 3) in terms of percentile (e.g., 50% or α=0.5) of the CDF over the full 3D sphere around the UE. CDF is quantitatively defined as follows:

$$CDF(\alpha) = \frac{\int_{\theta=0}^{\pi} \int_{\varphi=0}^{2\pi} \mathbb{I}(G_{realized}(w_c, \theta, \varphi) \leq \alpha)|sin\ (\theta)|d\theta d\varphi}{4\pi}$$

where $\mathbb{I}$ (.) is the identity function which returns the argument at the output if the argument's logic is true and 0 otherwise. To rephrase, the function $\mathbb{I}$ (.) returns $G_{realized}$ if $G_{realized}$ is either less than or equal to α. Otherwise, $\mathbb{I}$ (.) returns 0.

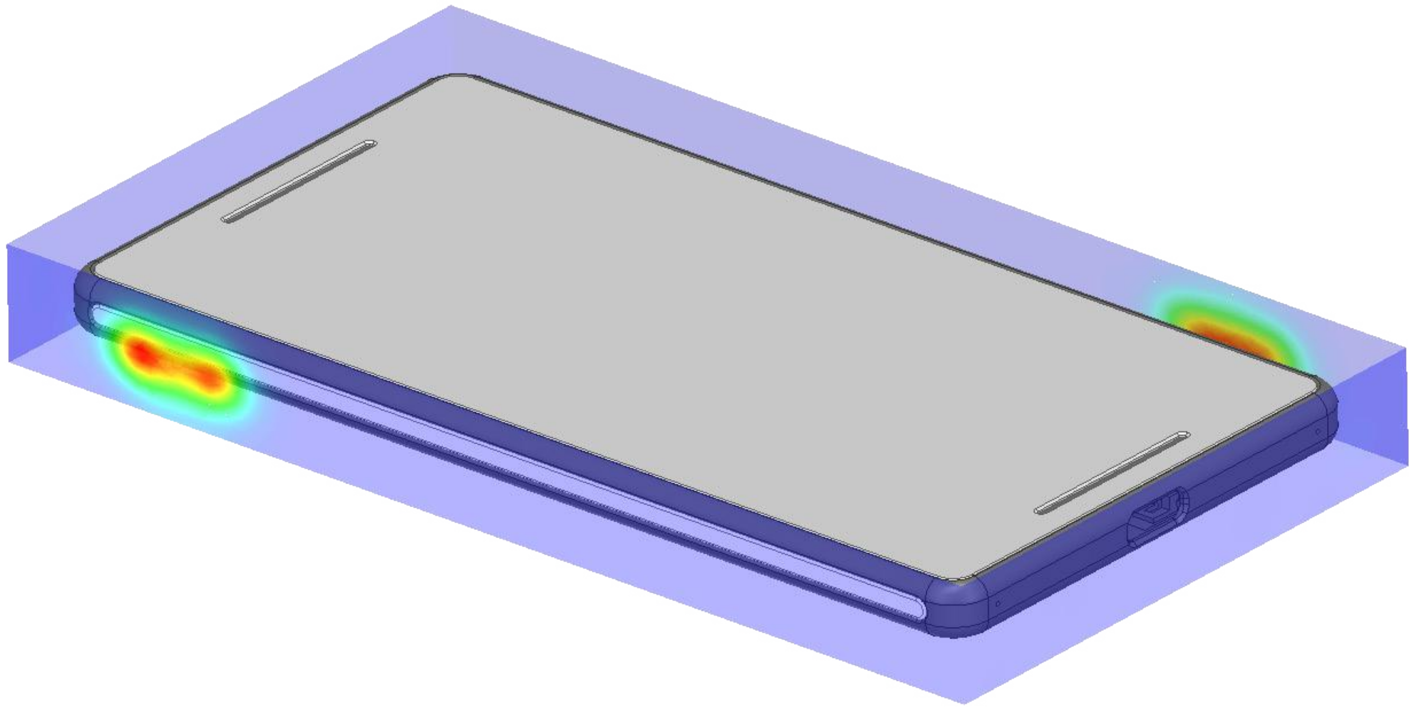

Figure 9. Power density plot (W/m2) @ 5mm offset from device

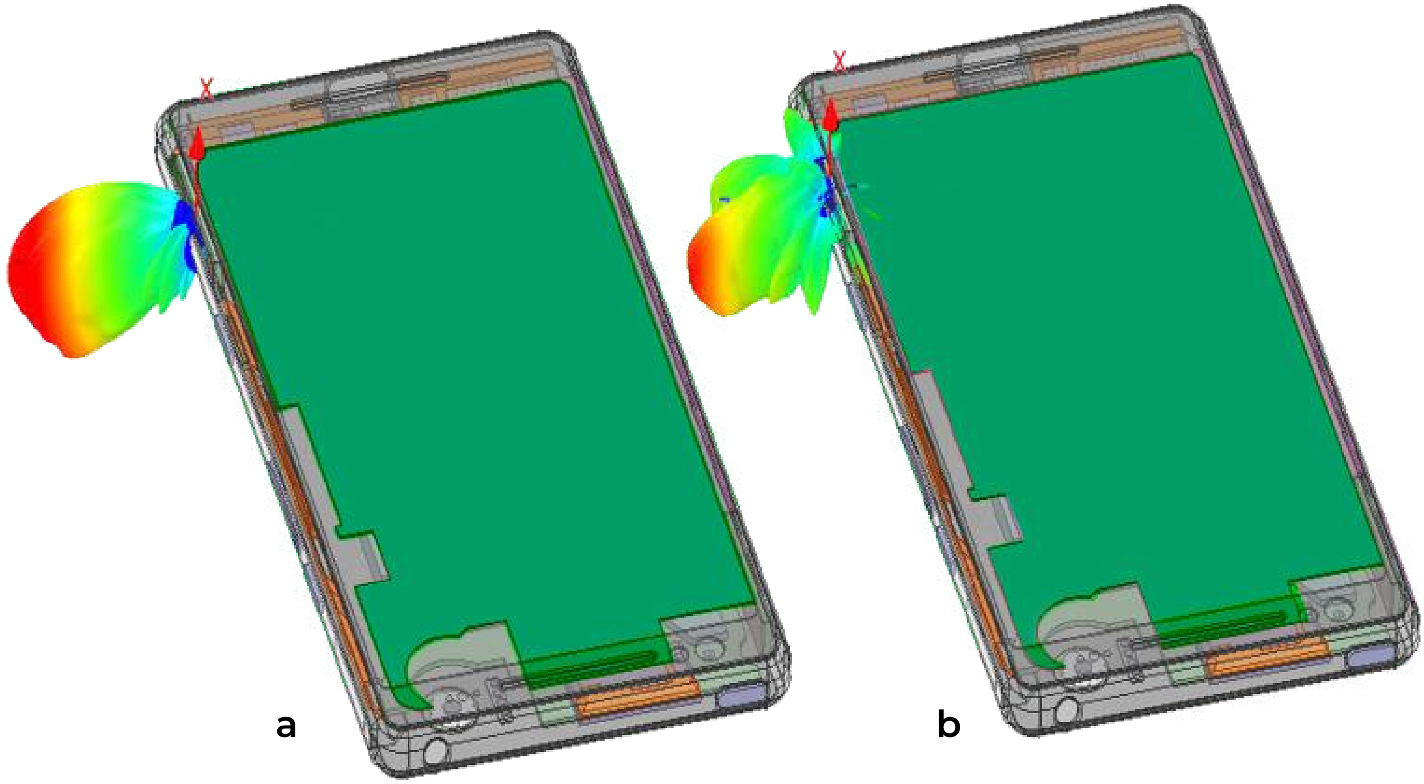

Figure 10. Radiation gain pattern (linear scale) for the designed mm-wave array embedded with phone body. Two different Beam ID or codewords, at 28 GHz (a) broadside with 8 dB realized gain, (b) 20 degrees off the broadside with 6.5 dB realized gain.

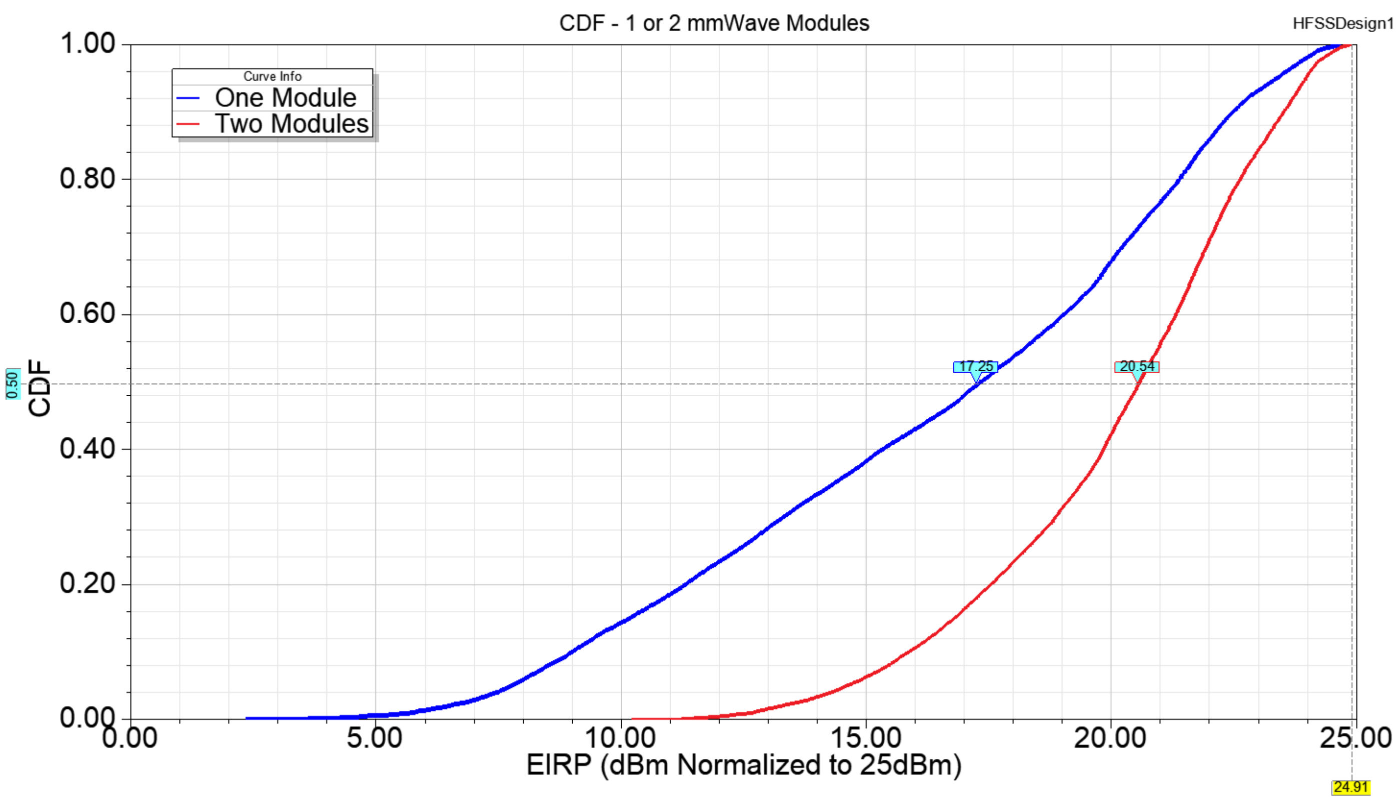

Figure 11. CDF curves for two scenarios: 1) UE with single mm-wave array (Array 1); 2) UE with both Array 1 and Array 2 (diversity array)

/ Analyzing Human Interactions

The final part of the UE design revolves around analyzing human interactions with the device and the effect on the antenna performance and efficiency.

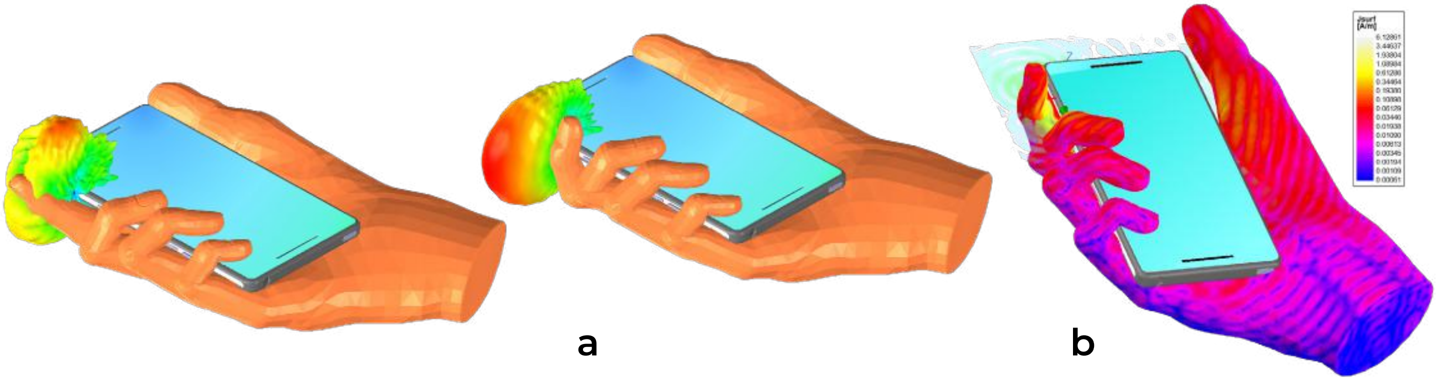

Figure 12. Human-device interaction with mm-wave array of a typical 5G UE, (a) far-field, (b) near-field (simulated in Ansys HFSS)

Ansys HFSS has a library of human body models which are used for the analysis of the hand-held device. The hand model can also be imported into HFSS from other CAD tools such as Ansys SpaceClaim or 3D graphics toolsets. HFSS has a rich library of material properties that are well-suited to model a human body and its composition. For instance, using materials such as skin, fat, bone, etc., in HFSS, a human body is explicitly modeled.

Simulation is performed for the hand-held smartphone design to understand the effects of human-device interactions. The analysis provides insights on the impact of the hand location, placement and its vicinity to the mm-wave array in its near-field and radiated far-field. **Figure 12** shows the results of the analysis when the phone is held in two different positions. When the hand is close to the array, the radiation pattern is affected. The results depict the importance of using diversity arrays in a UE design for improved performance. The final part of the user equipment design revolves around analyzing human interactions with the device and the effect on the antenna performance.

/ Conclusion

This paper described the potential of 5G and its challenges, emphasizing that accurate design and simulation of 5G end user devices are critical. The paper described a workflow for engineers to design 5G end user devices, improve their electromagnetic performance and also evaluate human-device interaction. The simulation results show that designing these UEs on Ansys HFSS improves their performance and efficiency. As expressly stated in the paper, the design and optimization of UE and microcell (or base station) cannot be optimally achieved in isolation. They depend on the communication channel between the UE and microcell. This interesting topic is resumed and explored in an ensuing paper, **"**How to Design 5G Base Station or Microcell Antenna Systems for 5G Wireless Networks.**"** Read the paper for a deeper insight into 5G base station (or microcell) array designs and the communication channel between the UE and base station.

References

[1] T. S. Rappaport et al., "Millimeter Wave Mobile Communications for 5G Cellular: It Will Work!," IEEE Access, vol. 1, pp. 335-349, 2013.

[2] Y. Huo, X. Dong and W. Xu, "5G Cellular User Equipment: From Theory to Practical Hardware Design," IEEE Access, vol. 5, pp. 13992-14010, 2017.

[3] M. Shafi et al., "5G: A Tutorial Overview of Standards, Trials, Challenges, Deployment, and Practice," IEEE Journal on Selected Areas in Communications, vol. 35, no. 6, pp. 1201-1221, June 2017.

[4] E. Dahlman et al., "5G Wireless Access: Requirements and Realization," IEEE Communications Magazine, vol. 52, no. 12, pp. 42-47, December 2014.

[5] V. Raghavan, M. Chi, M. A. Tassoudji, O. H. Koymen, and J. Li, "Antenna Placement and Performance Trad eoffs With Hand Blockage in Millimeter Wave Systems," IEEE Transactions on Communications, vol. 67, no. 4, pp. 3082-3096, April 2019.

[6] J. Mo et al., "Beam Codebook Design for 5G mmWave Terminals," IEEE Access, vol. 7, pp. 98387-98404, 2019.

[7] F. Croq and D. M. Pozar, "Millimeter Wave Design of Wide-band Aperture Coupled Stacked Microstrip An tennas," IEEE Trans. Antennas and Propagation, Vol. 39, No. 12, pp. 1770-1776, Dec. 1991.

[8] H. Oraizi and M. Fallahpour, "Sum, Difference and Shaped Beam Pattern Synthesis by Non-Uniform Spac ing and Phase Control," IEEE Transactions on Antennas and Propagation, vol. 59, no. 12, pp. 4505-4511, Dec. 2011.

[9] H. Oraizi and M. Fallahpour, "Nonuniformly Spaced Linear Array Design for the Specified Beamwidth/Sid elobe Level or Specified Directivity/Sidelobe Level with Coupling Consideration," Progress In Electromag netics Research M, Vol. 4, 185-209, 2008.

[10] A. Sligar, M. Raju, M. Ravenstahl, M. Commens, R. Petersson, S. Carpenter, J. Mologni, "Ansys 5G Antenna Solutions," Nov 2019.

[11] A. Sligar, M. Raju, M. Ravenstahl, M. Commens, S. Carpenter, J. Mologni, "Ansys 5G Mobile/UE Solutions," Nov 2019.

[12] Kezhong Zhao, Vineet Rawat, Seung-Cheol Lee, and Jin-Fa Lee, "A Domain Decomposition Method With Nonconformal Meshes for Finite Periodic and Semi-Periodic Structures," IEEE Trans. Antennas and Propa gation, Vol. 55, No. 9, pp. 2559-2570, Sept 2007.

Figure 13. Base Station or microcell. Read "How to Design 5G Base Station or Microcell Antenna Systems for 5G Wireless Networks" for more information.

Making meaningful impact, it drove us to start the business in 1995 and it has driven every project since. From designing advanced products and technologies to accelerating time to market, Boston Engineering thrives on solving tough client challenges and improving the way that people work and live.

Boston Engineering Corporation
300 Bear Hill Road
Waltham, MA 02451
781-466-8010

Visit www.boston-engineering.com for more information.